

**Exploring Potential of Adsorptive-Photocatalytic Molybdenum
Disulphide/Polyacrylonitrile (MoS₂/PAN) Nanofiber Coated Cellulose Acetate (CA)
Membranes**

Nur Shafiqah Jamaluddin^a, Nur Hashimah Alias^{a*}, Juhana Jaafar^b, Nur Hidayati Othman^a
Samitsu Sadaki^c, Fauziah Marpani^a, Woei Jye Lau^b

^a Department of Oil and Gas Engineering, School of Chemical Engineering, College of Engineering, Universiti Teknologi MARA, 40450 Shah Alam, Selangor, Malaysia

^b Advanced Membrane Technology Research Centre (AMTEC), Universiti Teknologi Malaysia, 81310 Skudai, Johor, Malaysia

^c National Institute for Materials Science, 1-2-1, Sengen, Tsukuba 305-0047, Japan

Corresponding author: nurhashimah@uitm.edu.my

ABSTRACT

Adsorptive electrospun nanofiber membranes have received remarkable attention as it could provide a great solution for the removal of organic contaminants in wastewater. However, the mechanical properties of nanofiber have limited their use in the pressure-driven filtration applications. In this study a dual-layered MoS₂/PAN adsorptive photocatalytic membrane was successfully fabricated using molybdenum disulphide/polyacrylonitrile (MoS₂/PAN) nanofiber coated porous cellulose acetate (CA) membranes. Flat sheet-CA membrane was first fabricated via phase inversion technique and subsequently coated with MoS₂/PAN nanofiber via electrospinning technique. Hot-press treatment was also applied on this dual-layered membrane to form stronger attachment between CA layer and MoS₂/PAN nanofiber layer. The physicochemical properties of the fabricated membranes were characterised using scanning electron microscopy (SEM), water contact angle (WCA) and porosity analysis, as well as tensile strength test. The membrane separation performance of the fabricated nanofiber membranes was evaluated in term of water flux and contaminant rejection using self-assembled cross-flow filtration system. The MoS₂/PAN-CA membrane demonstrated improved physicochemical and structural properties where WAC, porosity and mechanical strength increased up to 38% (44.0°), 25% (55%) and 56% (4.62 MPa), respectively as compared to CA membrane. Upon hot-pressed treatment at temperature 120 °C, pure water flux of MoS₂/PAN-CA membrane improved significantly at 36.3 Lm⁻²h⁻¹. Based on the results

obtained, it is possible to highlight this adsorptive-photocatalytic MoS₂/PAN-CA membrane as a promising candidate for effective treatment of organic micropollutants.

Keywords: *Electrospinning, electrospun nanofiber, MoS₂, adsorptive, membrane, filtration*

1. Introduction

Water pollution by organic pollutants has become a serious worldwide concern as it causes many harmful effects to the aquatic ecosystem and human health. The most typical organic pollutants that found in water and wastewater effluent are organic dyes and pesticides [1]. With the increasing of industrial activities which contribute to the destruction of water resource, it becomes urgent to develop an efficient treatment to eliminate the organic pollutants. Numerous treatment strategies have been applied including ion exchange, electrochemical reduction, chemical precipitation, adsorption and photocatalytic degradation. Among these approaches, photocatalytic degradation is regard as the most effective method to remove wide range of organic pollutants [2]. However, an additional cost and separation step like centrifugation is required in order to remove photocatalyst out from the system [3,4].

Fortunately, membrane separation technology provides a one-step treatment procedure, and has been considered as a new promising alternative for the removal of organic contaminants [5,6]. Presently, nanofiber membranes have been attracted growing attention because of their unique features such as large specific surface area, interconnected pores, flexible and high porosity [7]. Electrospinning has emerged as the most versatile technique to produce nanofiber with controllable diameters from nanometers to several micrometers [7,8]. Due to their unique properties, electrospun nanofiber membrane (ENM) was tremendously used for photocatalyst interphase to regenerate the spent photocatalysts hence overcome the limitation of photocatalytic process [9]. Polyacrylonitrile (PAN) polymer is one of the most common synthetic polymers that has been used as photocatalytic substrate during electrospinning [10]. PAN was categorized under non-toxic synthetic polymer which has low cost and provide excellent properties in terms of thermal stability, solvent resistance, environmental stable and small interfibrous pore size [3,11]. Moreover, PAN has high resistance towards UV light which make them applicable in photocatalytic degradation [12].

Recently, molybdenum disulfide (MoS₂) which categorised under photocatalytic nanomaterial group have received widespread attention in organic contaminants removal

recently due to their high electron conductivity, large surface area and rich of active sites [13–15]. Furthermore, MoS₂ has a satisfactory bandgap approximately 1.96 eV, which makes it as potential candidate for removing organic pollutants especially under UV light irradiation [16]. Theoretically, the S-Mo-S layer structure of MoS₂ sheet put S exposed on the surface, which provides high number of active sites for affinity adsorption [17,18]. The negatively charged surface of MoS₂ could enhance the adsorption of organic pollutant that have positively charged ions. Several researchers have proven the effectiveness of MoS₂ embedded in a solid matrix substrate for the removal of organic pollutants including methylene blue [19–21], rhodmine B[22], pyridine[23] and endocrine [24]. For instance, Zhao et al., [25] reported that the deposition of MoS₂ and polydopamine on ultrafiltration membrane can achieved 99 % rejection of methylene blue [19]. What is more, the incorporation MoS₂ into nanofiber membranes demonstrate excellent removal of organic pollutant even after third cycle of adsorption and desorption process [22].

Nevertheless, the development of MoS₂ embedded into nanofiber membrane for photocatalytic ENM still needs to be improved as the mechanical stability of ENM in pressure driven system is not satisfactory [26]. In addition, most of the previous works only focus on the fabrication and modification of photocatalytic membrane. There was very limited reported attempt to enhance the mechanical strength of photocatalytic ENM via coating assisted hot-press treatment technique. In this regard, this paper explored the potential of CA membrane as supporting layer for adsorptive photocatalytic MoS₂/PAN nanofiber due to their high mechanical strength, chemical resistance, low cost and bio-friendly [27,28]. The effect of hot press treatment at various temperature on the MoS₂/PAN nanofiber and CA membrane was investigate in order to achieve the most durable ENM. In addition, the characterization and analysis of morphology, water contact angle, porosity, tensile strength and water flux performance were also conducted and discussed thoroughly.

2. Methodology

2.1 Materials

Cellulose acetate (CA, MW= 30, 000 g/mol), Polyacrylonitrile (PAN, MW=150,000 g/mol) was used as polymer material for the preparation of composite membrane. Commercial molybdenum disulfide (MoS₂) powder with purity > 99% was used to synthesis MoS₂ nanofiber. N,N-dimethylformamide (DMF, 99%), was selected to be used as the solvent in preparation of nanofibrous composite membrane. All the chemicals were purchased from

Sigma Aldrich without further purification.

2.2 Fabrication of CA membrane

13g of CA powder was weighed and dissolved in 87g of DMF solvent at 27 °C for 24 hours. As CA completely dissolved and obtained a clear solution, the solution was degassed for 2h in ultrasonic bath in order to ensure there is no air bubbles in the solution. Then, the 13wt% CA solution was casted on a glass plate using glass rod. Consequently, the glass plate with casted CA solution was immersed in water bath at 25 °C, where the DMF and (water) can be exchange. After the phase inversion completed, the CA membrane was dried at room temperature for 24 hours before use.

2.3 Fabrication of nanofibers and nanofibers coated CA membrane

Initially, pure 10 wt.% PAN dope solution for electrospinning process was prepared as the control. On the other hand, MoS₂/PAN dope solution was prepared by mixing 1.9 wt.% MoS₂ in DMF and PAN. In detail, commercialized 2D MoS₂ was firstly dispersed into DMF and sonicate for 2 h. After that, PAN was added into the exfoliated MoS₂. The prepared PAN and MoS₂/PAN dope solutions were drawn directly on CA membrane using electrospinning technique. Typically, the spinning solution was filled in a plastic syringe before setting up the electrospinning parameters condition. The distance of the tip needle and ground collector was set at 18 cm and the rotating speed was constant at 180 rpm. Afterwards, the prepared solution was electrospun at 15 kV and feed flow rate of 1.0 ml/hr using 21G metallic needle. All the experiments were conducted at ambient temperature. Subsequently, the obtained PAN-CA membrane and MoS₂/PAN-CA membrane were dried for 24 hours at room temperature. Additionally, PAN nanofiber and MoS₂/PAN nanofibers without CA membrane layer were also fabricated using similar steps to distinguish their properties with the coated membrane.

2.3 Hot-pressed treatment

The dried composite of PAN-CA membrane and MoS₂/PAN-CA membrane was hot-pressed for 180 seconds. To investigate the suitable temperature for good attachment between nanofiber and flat-sheet membrane, the temperature for hot-press treatment of PAN-CA membrane and MoS₂/PAN-CA membrane was adjusted at two different degree (90 °C and 120 °C). The fabricated membrane with 90 °C hot-press treatment was briefly called as PAN-

CA@90 membrane. The overall process for MoS₂/PAN-CA membrane was illustrated in Figure 1.

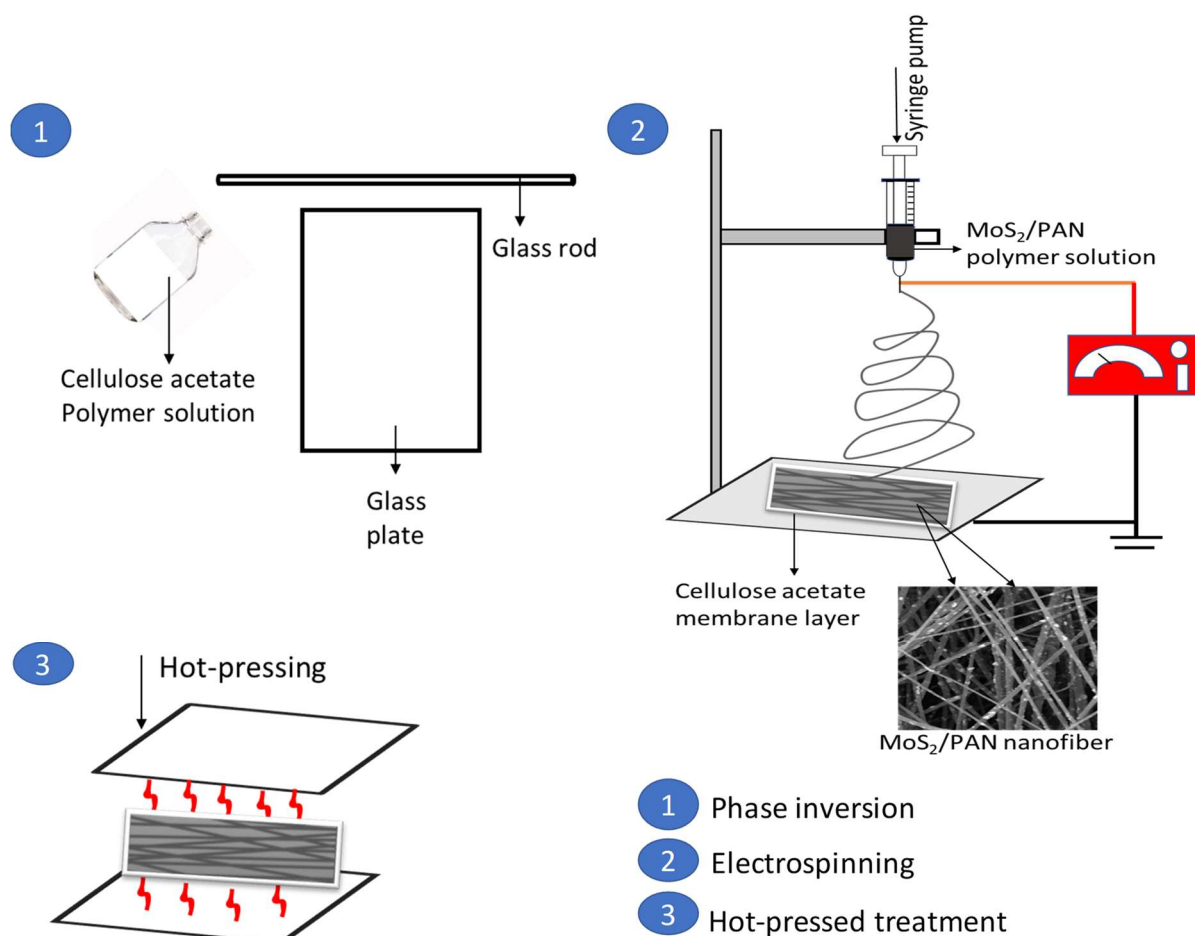


Figure 1: Schematic illustration for preparation step for MoS₂/PAN-CA membrane via phase inversion and electrospinning with hot-pressed treatment

2.5 Characterization of fabricated membranes

The top surface and cross-section morphologies of the fabricated membranes were observed by a Scanning Electron Microscope (Hitachi SU8020). All the membrane samples were snapped under liquid nitrogen for cross-sectional imaging. Then, the membranes were coated with a gold thin film. The membranes porosity was determined by dry-wet technique. The contact angle measurement was captured by contact angle meters at three different locations in order to minimize experimental error. The probe liquid used in contact angle measurement was de-ionized water. Before proceed with tensile test, the membrane thickness of the fabricated membrane was measured using micrometre screw gauge and was cut into the size of 60mm and 10mm. The tensile property of membrane was tested on a Shimadzu tensile

tester (ASTM D 882) at ambient temperature. The tensile stress and strain parameters of membrane were performed two times to get an average data.

2.6 Water flux performance

The performance of CA membrane and MoS₂/PAN-CA membrane in terms of water flux was performed using a cross-flow filtration setup as shown in Figure 2. 1000 ml distilled water will pass through a 47mm of the fabricated membrane at a transmembrane pressure of 1 bar. The feed pure water solution was recirculated for at least 3 times to obtain accurate reading. The water flux was calculated using Equation 1 [29].

$$W_f = \frac{V}{A \Delta t} \quad (1)$$

where W_f is the water flux ($L \cdot m^{-2} \cdot h^{-1}$), V is the volume (L) of the feed solution, A is the area (m^2) of the membrane, and t is the time (h).

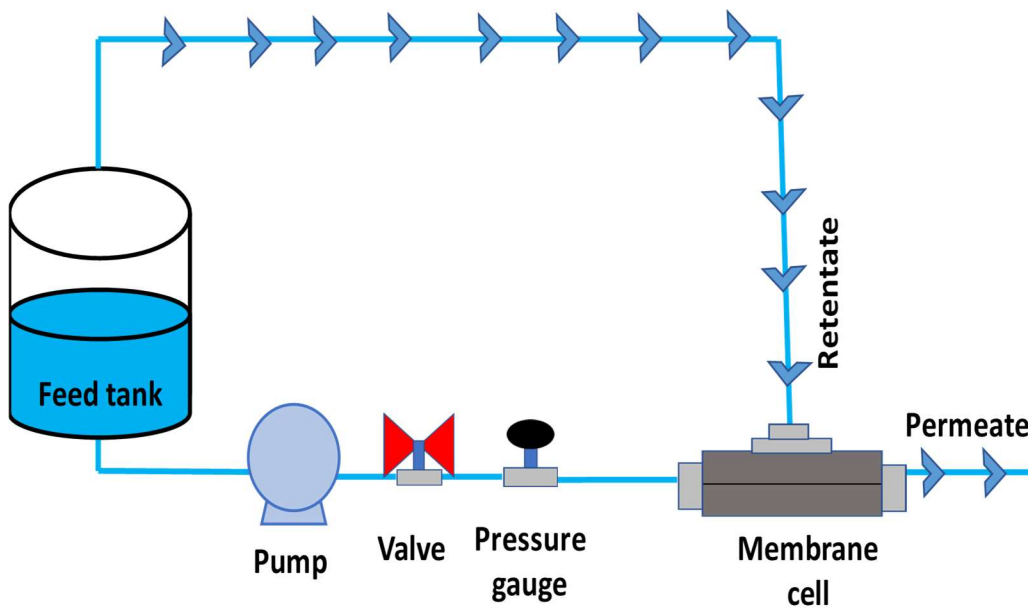


Figure 2: Schematic diagram of experimental setup for cross-flow filtration

3. Results and Discussion

3.1 Scanning Electron Microscopy

Scanning electron microscopy (SEM) was conducted to observed the nanofibers and polymeric skin membrane structure [30]. The SEM image of PAN nanofiber and MoS₂/PAN

nanofiber in dual magnification (1000k and 6000k) were shown in Figure 3.a)-d). As seen in Figure 3.a and b, PAN nanofiber presented a smooth, overlapping and uniform distribution of ultra-fine nanofiber, which presents a proper and successful electrospinning process. Generally, the overlapping structure of nanofiber represented the formation of interconnected pores [31]. However, the surface smoothness of PAN nanofiber was changed when 1.9 wt% exfoliated MoS₂ was added in 10 wt% PAN dope solution. In particular, a small amount of agglomerated MoS₂ was seen on the MoS₂ nanofiber surface as shown in Figure 3.b) and d). Yet, the composite nanofiber also displays an even pore diameter distribution, suggesting the incorporation of MoS₂ in the fabricated MoS₂/PAN nanofiber is uniform.

Theoretically, the agglomeration of MoS₂ was due to the high surface energy of the stacked layers of exfoliated MoS₂, which can act as driving force for crystal growth on the fiber surface [32,33]. Besides that, the incorporation of MoS₂ sheets also give a significant effect to the size of fiber diameter. The diameter of nanofibers was drastically increase from 594nm to 1020nm as MoS₂ were beneath on PAN nanofiber surface. Similar observation was reported on few past studies such as the incorporation of graphene oxide into PAN polymer solution for nanofiber formation via electrospinning was resulted to the increasing fiber diameter from 475 ± 53 nm to 1356 ± 267 nm [34]. Moreover, the loading of zeolite nanomaterials also reported have extremely changed the diameter of electrospun PVA nanofibers [35]. This phenomenon was mainly due to the changes in electrical conductivity and viscosity of polymer solutions that can attributed to the larger jet stretching [11].

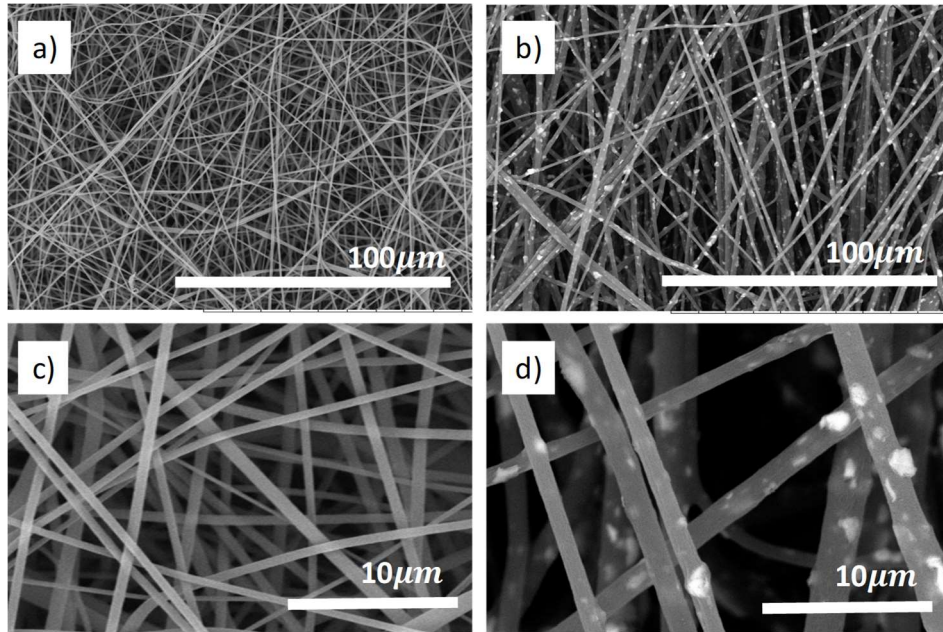


Figure 3: a) and b) Low and high magnification SEM images of PAN nanofiber, c) and d) Low and high magnification SEM images of MoS₂/PAN nanofiber.

Furthermore, the top surface and cross section of CA membrane, PAN-CA@90 membrane, PAN-CA membrane and MoS₂/PAN-CA membrane were also evaluated. The surface and cross-section image of CA membrane as support layer for nanofibers was shown in Figure 4.a) and b). Similar to other reported study [36], the fabricated CA membrane via phase inversion technique presented an asymmetric structure that consists of thin porous skin layer at the top surface and porous cross section with some macrovoids, which can provide a good mechanical strength for nanofibers. Figure 4.c) and d) showed the morphology of the fabricated PAN-CA@90 membrane. After being hot-pressed at 90°C, the roughness of PAN nanofiber was reduced without any substantial deformations. However, the cross section of the fabricated membrane clearly presented a severe detachment between CA membrane and PAN nanofiber. In comparison, the fabricated PAN-CA membrane displayed more rigid structure and attachment. The good attachment between substrate and nanofiber must be prioritize to prevent membrane from breakage. Hence, the hot pressed temperature for development of dual layered adsorptive photocatalytic MoS₂/PAN membrane was fixed at 120 °C and its surface morphology was shown in Figure 4.g) and h). From the Figure, it was observed that the fabricated MoS₂/PAN-CA membrane have higher surface roughness compared to the PAN-CA membrane This is due to the immobilization of MoS₂ nanomaterials. Even so, the successful immobilization of MoS₂ was expected can provide high affinity adsorption and photocatalytic degradation towards organic pollutants.

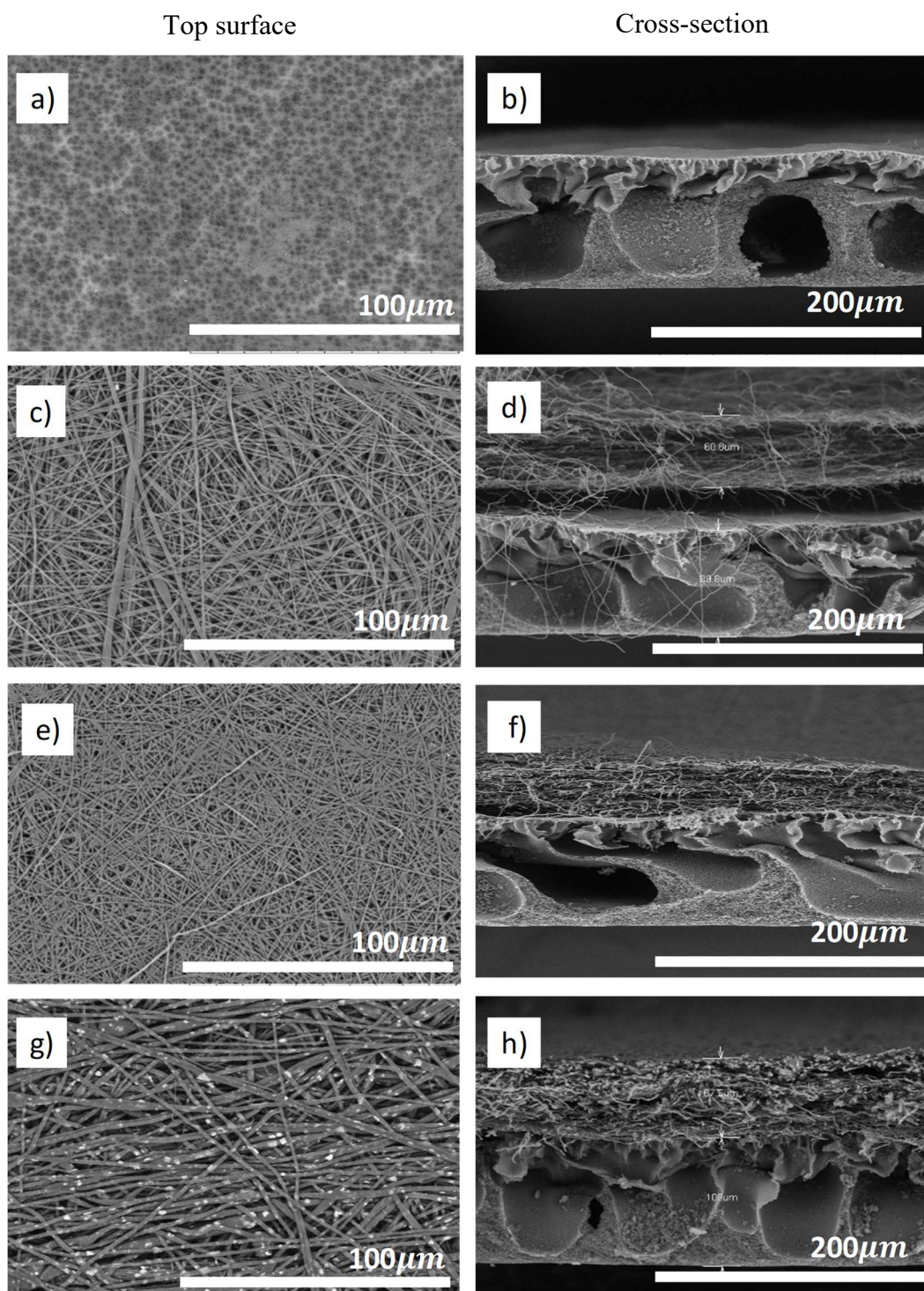


Figure 2: Top surface and cross section SEM micrographs a and b) CA membrane c and d) PAN-CA@90°C membrane e and f) PAN-CA membrane g and h) MoS₂/PAN-CA membrane.

3.4 Contact angle

Water contact angles for various fabricated membrane were presented in Figure 5. The contact angle of CA membrane was observed at 70.8°. This proved the hydrophilicity of asymmetric CA membrane by phase inversion. On the other hand, PAN nanofiber demonstrated hydrophobic characteristics with contact angle of 126.2°. The high hydrophobicity of nanofiber was due to the overlapping of nanofibers, which results in low contact area between nanofiber and water [37]. The contact angle of MoS₂/PAN nanofiber was slightly higher compared to the PAN nanofiber. The increase of hydrophobicity was mainly due to the incorporation of MoS₂ nanomaterials. Nevertheless, as fabricated nanofiber were coat on CA membrane subsequent with hot-press treatment, the hydrophobicity of PAN-CA membrane and MoS₂/PAN-CA membrane were extremely reduced and changed into the hydrophilic nature. Similar result was reported by Shahidul et al., [38] which found the hot-press membrane exhibited high hydrophilicity [38]. The low water contact angle for both hot-press membrane sample was due to the dense structure of composite membrane after being merge together [39]. Thus, it was expected that the contact angle of composite membrane will further decreases as the temperature of hot-pressed increases. However, it may minimize the direct contact of MoS₂ with organic pollutants.

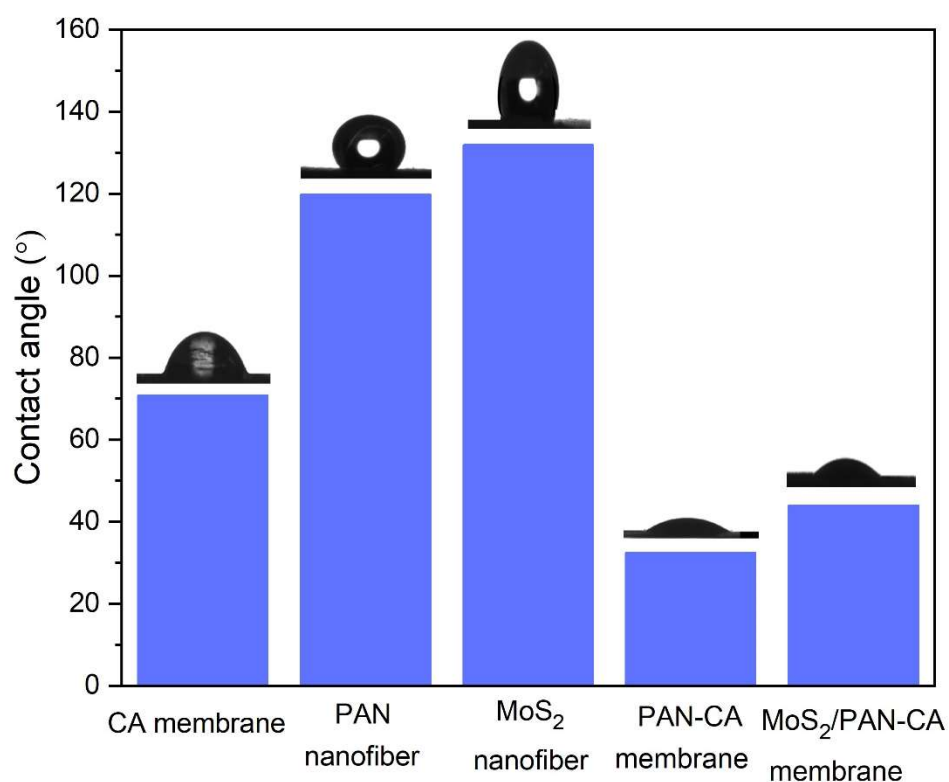


Figure 3: Contact angle analysis on different types of fabricated membranes.

3.5 Membrane porosity

The porosities of the fabricated membranes were calculated and summarized in Figure 6. The bar graph below showed that PAN nanofiber and MoS₂ nanofiber demonstrated higher porosity compared to CA membrane due to the existence of overlapping nanofiber structure. Nevertheless, the porosity of dual layered composite membranes were decreased after hot pressed-treatment as the pressure and temperature from hot-pressing treatment attributed to the increasing of nanofiber packing density and firmness, hence reduced the membrane porosity [40].

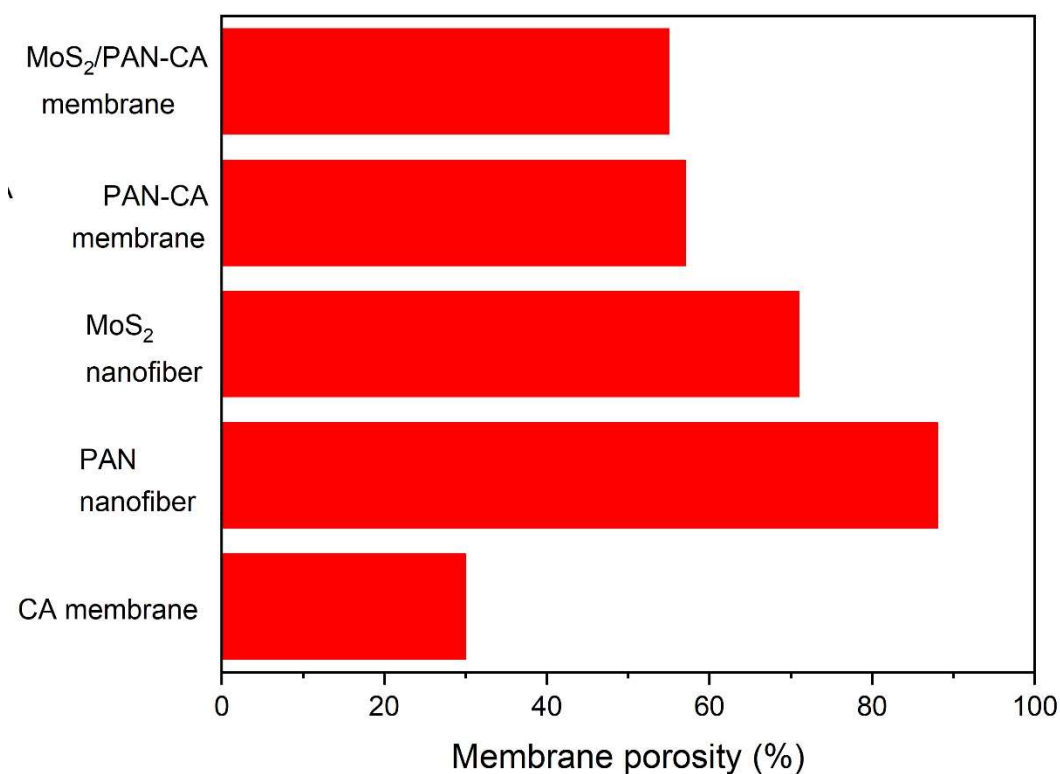


Figure 4: Percentage of membrane porosity on different types of fabricated membranes.

3.6 Tensile test

To further verified the firmness of the composite membrane after hot-pressed treatment, tensile test was performed. Figure 7 displays the tensile strength for CA membrane and MoS₂/PAN-CA membrane. It was clearly observed that the tensile strength of MoS₂/PAN-CA membrane was comparatively higher than CA membrane. The improvement in the tensile strength of the composite membrane was commonly due to the synergistic effects of CA membrane and MoS₂/PAN nanofiber [44,45]. The high strength of the adsorptive photocatalytic MoS₂/PAN-CA membrane was also due to the firm attachment of the

composite membrane after being hot-pressed. This finding was supported by photograph images of MoS₂/PAN-CA membrane and MoS₂/PAN nanofiber in dry and wet condition as depicted in Figure 8. From the Figure, MoS₂/PAN-CA membrane was able to maintain its mechanical stability in both conditions. On the other hand, uncoated nanofibers, MoS₂/PAN nanofiber displayed unrigid shape after being immersed with water.

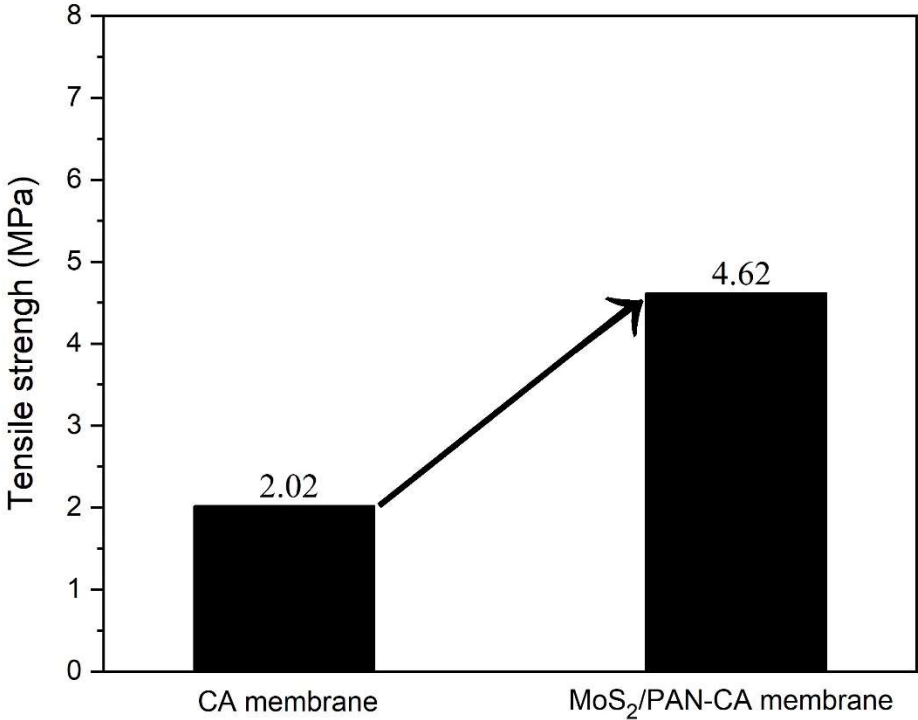


Figure 5: Tensile test analysis result on CA membrane and PAN-CA membrane.

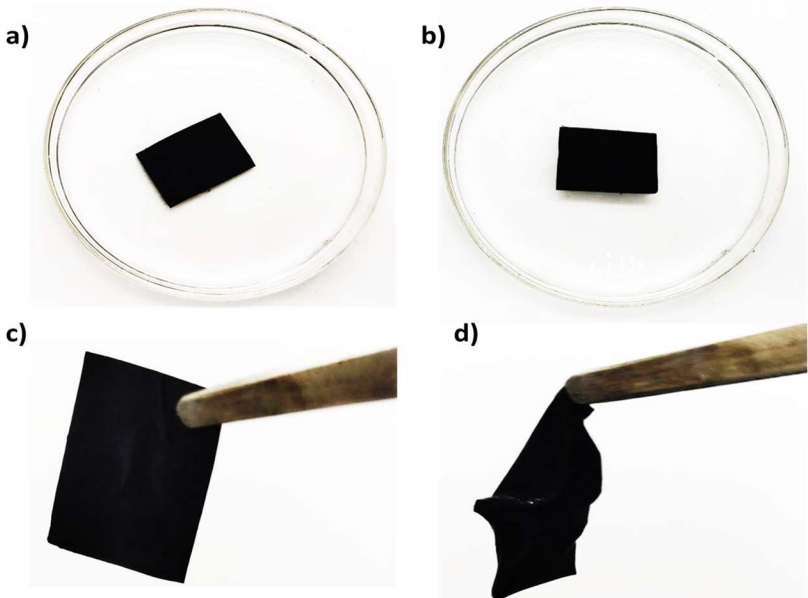


Figure 8: Photographs images of a) dry MoS₂/PAN nanofiber b) dry MoS₂/PAN-CA membrane c) wet MoS₂/PAN nanofiber d) dry MoS₂/PAN-CA membrane.

3.7 Water flux analysis

The pure water flux result of the fabricated membrane was depicted in Figure 9. Compared to CA membrane, the pure water flux of MoS₂/PAN-CA membrane enhanced approximately 10% of membrane pure water flux. This pure water flux improvement was in tune with the results reported in Figure 5 that revealed the MoS₂/PAN-CA membrane increased the membrane hydrophilicity. Generally, the membrane with high hydrophilicity properties could attract high amount of water molecules during filtration, which can increase the water permeation or water flux [41,42].

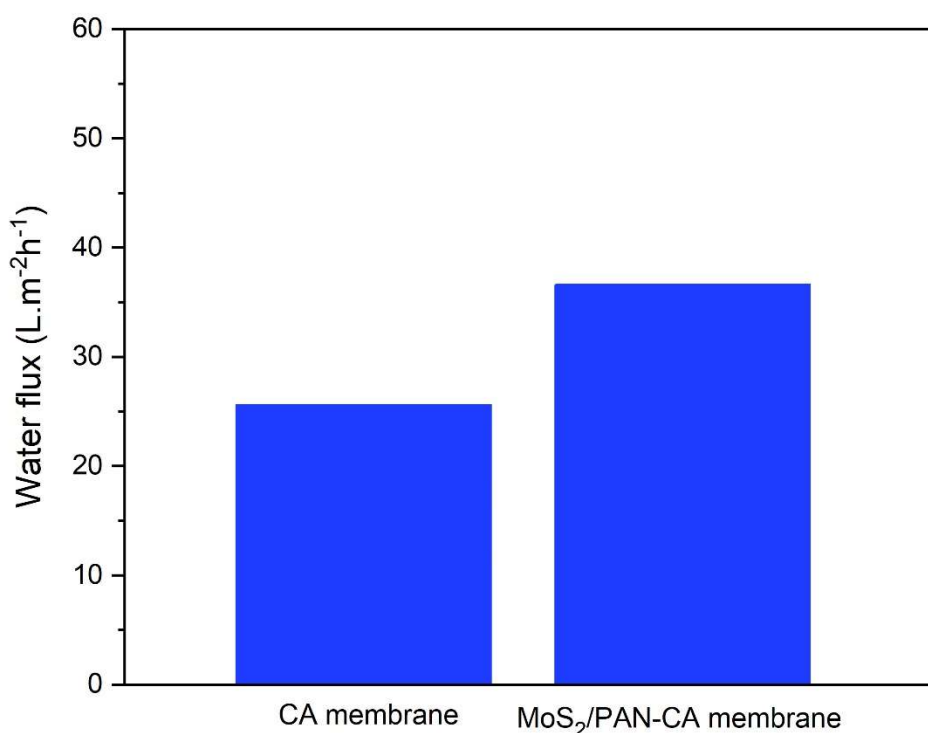


Figure 9: Water flux analysis on CA membrane and MoS₂/PAN-CA membrane.

4. Conclusion

MoS₂/PAN-CA membrane was successfully fabricated by electrospinning coating assisted hot-press treatment technique. The morphology and durable properties of the fabricated membrane were confirmed by several analysis such as SEM, water contact angle, porosity and tensile test. The SEM images of MoS₂/PAN-CA membrane displayed a uniform and bead-free MoS₂/PAN nanofiber whereas CA membrane demonstrated a thin skin layer with a porous structure. SEM image suggested that the hot-pressed treatment temperature was more favourable at 120°C. The water flux of CA membrane increased from 26% to 36% as it coated with hot-press nanofibers during electrospinning. The increment in water flux was due

to the enhancement of membrane porosity and hydrophilicity. Tensile test result proved that MoS₂/PAN-CA membrane demonstrated 4.62 MPa tensile strength, which is much higher compare to the flat-sheet CA membrane, 2.02 MPa. The successful incorporation of MoS₂ and the high mechanical properties of the composite membrane was expected can be a potential adsorptive photocatalytic membrane for high removal of various organic pollutants in water and wastewater.

Acknowledgement

The authors were gratefully acknowledged Malaysia Ministry of Higher Education (MOHE) for the FRGS research funding (600-IRMI/FRGS 5/3 (441/2019)). NSJ would like to thank Advanced Membrane Technology Research Centre (AMTEC), Universiti Teknologi Malaysia (UTM), Malaysia for the AMTEC fellowship program awarded.

References

- [1] F. Lu, D. Astruc, Nanocatalysts and other nanomaterials for water remediation from organic pollutants, *Coord. Chem. Rev.* 408 (2020) 213180. <https://doi.org/10.1016/J.CCR.2020.213180>.
- [2] R.S. Sutar, R.P. Barkul, M.K. Patil, Sunlight Assisted Photocatalytic Degradation of Different Organic Pollutants and Simultaneous Degradation of Cationic and Anionic Dyes Using Titanium and Zinc Based Nanocomposites, *J. Mol. Liq.* (2021) 117191. <https://doi.org/10.1016/J.MOLLIQ.2021.117191>.
- [3] A. Almasian, M. Giahi, G.C. Fard, S.A. Dehdast, L. Maleknia, Removal of heavy metal ions by modified PAN/PANI-nylon core-shell nanofibers membrane: Filtration performance, antifouling and regeneration behavior, *Chem. Eng. J.* 351 (2018) 1166–1178. <https://doi.org/10.1016/j.cej.2018.06.127>.
- [4] N.H. Alias, J. Jaafar, S. Samitsu, T. Matsuura, A.F. Ismail, M.H.D. Othman, M.A. Rahman, N.H. Othman, N. Abdullah, S.H. Paiman, N. Yusof, F. Aziz, Photocatalytic nanofiber-coated alumina hollow fiber membranes for highly efficient oilfield

- produced water treatment, *Chem. Eng. J.* 360 (2019) 1437–1446.
<https://doi.org/10.1016/J.CEJ.2018.10.217>.
- [5] G. Liu, K. Han, Y. Zhou, H. Ye, X. Zhang, J. Hu, X. Li, Facile Synthesis of Highly Dispersed Ag Doped Graphene Oxide/Titanate Nanotubes as a Visible Light Photocatalytic Membrane for Water Treatment, *ACS Sustain. Chem. Eng.* 6 (2018) 6256–6263. <https://doi.org/10.1021/ACSSUSCHEMENG.8B00029>.
- [6] N. Abdullah, N. Yusof, W.J. Lau, J. Jaafar, A.F. Ismail, Recent trends of heavy metal removal from water/wastewater by membrane technologies, *J. Ind. Eng. Chem.* 76 (2019) 17–38. <https://doi.org/10.1016/j.jiec.2019.03.029>.
- [7] H. Lee, I.S. Kim, Nanofibers: Emerging Progress on Fabrication Using Mechanical Force and Recent Applications, *Polym. Rev.* 58 (2018) 688–716.
<https://doi.org/10.1080/15583724.2018.1495650>.
- [8] J.P. Fan, J.J. Luo, X.H. Zhang, B. Zhen, C.Y. Dong, Y.C. Li, J. Shen, Y.T. Cheng, H.P. Chen, A novel electrospun B-CD/CS/PVA nanofiber membrane for simultaneous and rapid removal of organic micropollutants and heavy metal ions from water, *Chem. Eng. J.* 378 (2019) 122232. <https://doi.org/10.1016/j.cej.2019.122232>.
- [9] A.M. Nasir, N. Awang, J. Jaafar, A.F. Ismail, M.H.D. Othman, M. A. Rahman, F. Aziz, M.A. Mat Yajid, Recent progress on fabrication and application of electrospun nanofibrous photocatalytic membranes for wastewater treatment: A review, *J. Water Process Eng.* 40 (2021) 101878. <https://doi.org/10.1016/j.jwpe.2020.101878>.
- [10] L.D. Tijing, M. Yao, J. Ren, C. Park, Á.E.Á. Desalination, *Nanofibers for Water and Wastewater Treatment : Recent Advances and Developments*, 2019.
- [11] S. Deng, X. Liu, J. Liao, H. Lin, F. Liu, PEI modified multiwalled carbon nanotube as a novel additive in PAN nanofiber membrane for enhanced removal of heavy metal ions, *Chem. Eng. J.* 375 (2019) 122086. <https://doi.org/10.1016/j.cej.2019.122086>.

- [12] M. Romay, N. Diban, M.J. Rivero, A. Urriaga, I. Ortiz, Critical Issues and Guidelines to Improve the Performance of Photocatalytic Polymeric Membranes, *Catalysts*. 10 (2020) 570. <https://doi.org/10.3390/catal10050570>.
- [13] W. Cao, Y. Zhang, Z. Shi, T. Liu, X. Song, L. Zhang, P. Keung Wong, Z. Chen, Boosting the adsorption and photocatalytic activity of carbon fiber/MoS₂-based weavable photocatalyst by decorating UiO-66-NH₂ nanoparticles, *Chem. Eng. J.* (2020) 128112. <https://doi.org/10.1016/j.cej.2020.128112>.
- [14] C. Liu, F. Jia, Q. Wang, B. Yang, S. Song, Two-dimensional molybdenum disulfide as adsorbent for high-efficient Pb(II) removal from water, *Appl. Mater. Today*. 9 (2017) 220–228. <https://doi.org/10.1016/j.apmt.2017.07.009>.
- [15] F. Jia, K. Sun, B. Yang, X. Zhang, Q. Wang, S. Song, Defect-rich molybdenum disulfide as electrode for enhanced capacitive deionization from water, *Desalination*. 446 (2018) 21–30. <https://doi.org/10.1016/j.desal.2018.08.024>.
- [16] L. Zhang, L. Wu, Z. Feng, Q. Meng, Y. Li, T. Duan, Adopting sulfur-atom sharing strategy to construct CoS₂/MoS₂ heterostructure on three-dimensional nitrogen-doped graphene aerogels: A novel photocatalyst for wastewater treatment, *J. Environ. Chem. Eng.* (2020) 104771. <https://doi.org/10.1016/j.jece.2020.104771>.
- [17] Y.-C. Chen, A.-Y. Lu, P. Lu, X. Yang, C.-M. Jiang, M. Mariano, B. Kaehr, O. Lin, A. Taylor, I.D. Sharp, L.-J. Li, S.S. Chou, V. Tung, Structurally Deformed MoS₂ for Electrochemically Stable, Thermally Resistant, and Highly Efficient Hydrogen Evolution Reaction, *Adv. Mater.* 29 (2017) 1703863. <https://doi.org/10.1002/adma.201703863>.
- [18] X. Li, K. Peng, Hydrothermal synthesis of MoS₂ nanosheet/palygorskite nanofiber hybrid nanostructures for enhanced catalytic activity, *Appl. Clay Sci.* 162 (2018) 175–181. <https://doi.org/10.1016/j.clay.2018.06.015>.

- [19] H. Zhao, G. Liu, M. Zhang, H. Liu, M. Zhang, L. Zhou, J. Gao, Y. Jiang, Bioinspired modification of molybdenum disulfide nanosheets to prepare a loose nanofiltration membrane for wastewater treatment, *J. Water Process Eng.* 40 (2021). <https://doi.org/10.1016/J.JWPE.2020.101759>.
- [20] J. Zhou, Z. Qin, T. Liu, Y. Ma, Q. An, H. Guo, Fabrication of mos₂/polyelectrolyte composite membrane on ceramic tube with enhanced nanofiltration performance, *Desalin. Water Treat.* 156 (2019) 46–51. <https://doi.org/10.5004/DWT.2019.24256>.
- [21] R. Schneider, M.H.M. Facure, A.D. Alvarenga, P.A.M. Chagas, D.M. dos Santos, D.S. Correa, Dye Adsorption Capacity of MoS₂ Nanoflakes Immobilized on Poly(lactic acid) Fibrous Membranes, *ACS Appl. Nano Mater.* 4 (2021) 4881–4894. <https://doi.org/10.1021/ACSANM.1C00442>.
- [22] Y. Lu, Y. Fang, X. Xiao, S. Qi, C. Huan, Y. Zhan, H. Cheng, G. Xu, Petal-like molybdenum disulfide loaded nanofibers membrane with superhydrophilic property for dye adsorption, *Colloids Surfaces A Physicochem. Eng. Asp.* 553 (2018) 210–217. <https://doi.org/10.1016/J.COLSURFA.2018.05.056>.
- [23] L.J. Fang, J.H. Chen, J.M. Wang, W.W. Lin, X.G. Lin, Q.J. Lin, Y. He, Hydrophobic Two-Dimensional MoS₂ Nanosheets Embedded in a Polyether Copolymer Block Amide (PEBA) Membrane for Recovering Pyridine from a Dilute Solution, *ACS Omega.* 6 (2021) 2675–2685. <https://doi.org/10.1021/ACSOMEGA.0C04852>.
- [24] R. Dai, H. Han, T. Wang, X. Li, Z. Wang, Enhanced removal of hydrophobic endocrine disrupting compounds from wastewater by nanofiltration membranes intercalated with hydrophilic MoS₂ nanosheets: Role of surface properties and internal nanochannels, *J. Memb. Sci.* 628 (2021) 119267. <https://doi.org/10.1016/J.MEMSCI.2021.119267>.
- [25] R. Mukherjee, P. Bhunia, S. De, Impact of graphene oxide on removal of heavy metals using mixed matrix membrane, *Chem. Eng. J.* 292 (2016) 284–297.

- <https://doi.org/10.1016/j.cej.2016.02.015>.
- [26] F. Yalcinkaya, B. Yalcinkaya, A. Pazourek, J. Mullerova, M. Stuchlik, J. Maryska, Surface Modification of Electrospun PVDF/PAN Nanofibrous Layers by Low Vacuum Plasma Treatment, *Int. J. Polym. Sci.* 2016 (2016). <https://doi.org/10.1155/2016/4671658>.
- [27] H.Y. Choi, J.H. Bae, Y. Hasegawa, S. An, I.S. Kim, H. Lee, M. Kim, Thiol-functionalized cellulose nanofiber membranes for the effective adsorption of heavy metal ions in water, *Carbohydr. Polym.* 234 (2020) 115881. <https://doi.org/10.1016/j.carbpol.2020.115881>.
- [28] W. Li, T. Li, G. Li, L. An, F. Li, Z. Zhang, Electrospun H4SiW12O40/cellulose acetate composite nanofibrous membrane for photocatalytic degradation of tetracycline and methyl orange with different mechanism, *Carbohydr. Polym.* 168 (2017) 153–162. <https://doi.org/10.1016/j.carbpol.2017.03.079>.
- [29] N.H. Alias, J. Jaafar, S. Samitsu, T. Matsuura, A.F. Ismail, M.H.D. Othman, M.A. Rahman, N.H. Othman, N. Abdullah, S.H. Paiman, N. Yusof, F. Aziz, Photocatalytic nanofiber-coated alumina hollow fiber membranes for highly efficient oilfield produced water treatment, *Chem. Eng. J.* 360 (2019) 1437–1446. <https://doi.org/10.1016/j.cej.2018.10.217>.
- [30] M.A. Silva, E. Belmonte-Reche, M.T.P. de Amorim, Morphology and water flux of produced cellulose acetate membranes reinforced by the design of experiments (DOE), *Carbohydr. Polym.* 254 (2021) 117407. <https://doi.org/10.1016/j.carbpol.2020.117407>.
- [31] H. Zeng, Z. Yu, L. Shao, X. Li, M. Zhu, Y. Liu, X. Feng, X. Zhu, Ag₂CO₃@UiO-66-NH₂ embedding graphene oxide sheets photocatalytic membrane for enhancing the removal performance of Cr(VI) and dyes based on filtration, *Desalination.* 491 (2020) 114558. <https://doi.org/10.1016/j.desal.2020.114558>.

- [32] X. Yu, H.S. Park, Synthesis and characterization of electrospun PAN/2D MoS₂ composite nanofibers, *J. Ind. Eng. Chem.* 34 (2016) 61–65. <https://doi.org/10.1016/j.jiec.2015.10.030>.
- [33] A.A. Hamad, M.S. Hassouna, T.I. Shalaby, M.F. Elkady, M.A. Abd Elkawi, H.A. Hamad, Electrospun cellulose acetate nanofiber incorporated with hydroxyapatite for removal of heavy metals, *Int. J. Biol. Macromol.* 151 (2020) 1299–1313. <https://doi.org/10.1016/j.ijbiomac.2019.10.176>.
- [34] Z.Q. Feng, X. Yuan, T. Wang, Porous polyacrylonitrile/graphene oxide nanofibers designed for high efficient adsorption of chromium ions (VI) in aqueous solution, *Chem. Eng. J.* 392 (2020) 123730. <https://doi.org/10.1016/j.cej.2019.123730>.
- [35] L.R. Rad, A. Momeni, B.F. Ghazani, M. Irani, M. Mahmoudi, B. Noghreh, Removal of Ni²⁺ and Cd²⁺ ions from aqueous solutions using electrospun PVA/zeolite nanofibrous adsorbent, *Chem. Eng. J.* 256 (2014) 119–127. <https://doi.org/10.1016/j.cej.2014.06.066>.
- [36] A.M. Pandele, F.E. Comanici, C.A. Carp, F. Miculescu, S.I. Voicu, V.K. Thakur, B.C. Serban, Synthesis and characterization of cellulose acetate-hydroxyapatite micro and nano composites membranes for water purification and biomedical applications, *Vacuum.* 146 (2017) 599–605. <https://doi.org/10.1016/j.vacuum.2017.05.008>.
- [37] L.D. Tijjing, Y.C. Woo, M.A.H. Jahir, J.S. Choi, H.K. Shon, A novel dual-layer bicomponent electrospun nanofibrous membrane for desalination by direct contact membrane distillation, *Chem. Eng. J.* 256 (2014) 155–159. <https://doi.org/10.1016/j.cej.2014.06.076>.
- [38] M.S. Islam, S. Sultana, M.S. Rahaman, Electrospun nylon 6 microfiltration membrane for treatment of brewery wastewater, in: *AIP Conf. Proc.*, American Institute of Physics Inc., 2016: p. 060017. <https://doi.org/10.1063/1.4958458>.

- [39] M. Kumar, J. Jaafar, Preparation and characterization of TiO₂ nanofiber coated PVDF membrane for softdrink wastewater treatment, *Environ. Ecosyst. Sci.* 2 (2018) 35–38. <https://doi.org/10.26480/ees.02.2018.35.38>.
- [40] Z. Wang, R. Sahadevan, C. Crandall, T.J. Menkhaus, H. Fong, Hot-pressed PAN/PVDF hybrid electrospun nanofiber membranes for ultrafiltration, *J. Memb. Sci.* 611 (2020) 118327. <https://doi.org/10.1016/j.memsci.2020.118327>.
- [41] Q. Liu, S. Huang, Y. Zhang, S. Zhao, Comparing the antifouling effects of activated carbon and TiO₂ in ultrafiltration membrane development, *J. Colloid Interface Sci.* 515 (2018) 109–118. <https://doi.org/10.1016/j.jcis.2018.01.026>.
- [42] Y. Ibrahim, V. Naddeo, F. Banat, S.W. Hasan, Preparation of novel polyvinylidene fluoride (PVDF)-Tin(IV) oxide (SnO₂) ion exchange mixed matrix membranes for the removal of heavy metals from aqueous solutions, *Sep. Purif. Technol.* 250 (2020) 117250. <https://doi.org/10.1016/j.seppur.2020.117250>.